Development of a Flow Cytometry-Based Whole-Blood Prognostic Immune Signature in Metastatic Cancer Patients treated with immune checkpoint inhibitors

Jian-Guo Zhou*[,1,2,3], Anna-Jasmina Donaubauer*[,1,2], Benjamin Frey[1,2], Ina Becker[1,2], Sandra Rutzner[1,2], Markus Eckstein[2,4], Roger Sun[5,6], Hu Ma[3], Philipp Schubert[1,2], Claudia Schweizer[1,2], Rainer Fietkau[1,2], Eric Deutsch[5,6], Udo S. Gaipl[#,1,2,+], Markus Hecht[#,1,2]

[1] Department of Radiation Oncology, Universitätsklinikum Erlangen, Erlangen, Germany

[2] Comprehensive Cancer Center Erlangen-EMN, Erlangen, Germany

[3] Department of Oncology, The second affiliated Hospital of Zunyi Medical University, Zunyi, China

[4] Institute of Pathology, Universitätsklinikum Erlangen, Friedrich-Alexander-Universität Erlangen-Nürnberg, Erlangen, Germany

[5] Department of Radiation Oncology, Gustave Roussy-CentraleSupélec-TheraPanacea Center of Artificial Intelligence in Radiation Therapy and Oncology, Gustave Roussy, Villejuif, France

[6] Université Paris-Saclay, INSERM1030 Radiothérapie Moléculaire,Villejuif France

* JGZ and AJD contributed equally as first authors

# USG and MH contributed equally as senior authors

Jian-Guo Zhou: jianguo.zhou@fau.de

Anna-Jasmina Donaubauer: Anna-Jasmina.Donaubauer@uk-erlangen.de

Benjamin Frey: Benjamin.Frey@uk-erlangen.de

Ina Becker: Ina.Becker@uk-erlangen.de

Sandra Rutzner: sandra.rutzner@uk-erlangen.de

Markus Eckstein: markus.eckstein@uk-erlangen.de

Roger Sun: ROGER.SUN@gustaveroussy.fr

Hu Ma: mahuab@163.com

Philipp Schubert: Philipp.Schubert@uk-erlangen.de

Claudia Schweizer: Claudia.Schweizer@uk-erlangen.de

Rainer Fietkau: Rainer.Fietkau@uk-erlangen.de

Eric Deutsch: Eric.DEUTSCH@gustaveroussy.fr

Udo S. Gaipl: udo.gaipl@uk-erlangen.de

Markus Hecht: markus.hecht@uk-erlangen.de

+ Corresponding author:

Prof. Dr. Udo S. Gaipl

Department of Radiation Oncology, Universitätsklinikum Erlangen

Friedrich-Alexander-Universität Erlangen-Nürnberg (FAU)

Universitätsstraße 27, 91054 Erlangen, Germany

Tel.: +49 9131 85 44258; Fax: +49 9131 85 39335

E-mail address: udo.gaipl@uk-erlangen.de.

Abbreviations

AUC: The area under the ROC curve

CI: Confidence interval

C-index: Concordance index

CTLA-4: Cytotoxic T lymphocyte antigen-4

ECOG: Eastern Cooperative Oncology Group

FCBPS: Flow cytometry- based whole-blood prognostic signature

HNSCC: Head and neck squamous cell carcinoma

HR: Hazard ratios

ICI: Immune checkpoint inhibitors

IPT: immunophenotyping

LASSO: Least absolute shrinkage and selection operator

NE: Not estimate

NK cells: Natural killer cells

NKT cells: Natural killer T cells

NSCLC: Non-small cell lung cancer

OS: Overall survival

PBMCs: Peripheral blood mononuclear cells

PD-1: Programmed cell death protein 1

pDCs: Plasmacytoid Dendritic Cells

PD-L1: Programmed cell death ligand 1

PFS: Progression free survival

RECIST: Response Evaluation Criteria in Solid Tumors

ROC: Receiver operating characteristic

TMB: Tumor mutational burden

Tregs: Regulatory T Cells

Abstract

Recent biomarker research focuses on early immunological changes to predict treatment response to immune checkpoint inhibitors (ICI). Within this prospective ST-ICI trial, pre-planned biomarker analysis was performed and we developed a flow cytometry-based whole-blood prognostic immune signature (FCBPS) to predict overall survival (OS) benefit of cancer patients treated with ICI. For this, fifty-four immune cell subsets were analyzed in the patients' peripheral blood before the second administration of the ICI. Patients were randomly allocated to a training and validation cohort. Univariate Cox proportional hazards regression analysis and LASSO Cox model were used to develop a predictive and prognostic signature. 104 patients were prospectively enrolled. 89 patients provided blood samples. The identified FCBPS signature bases on five immune cell subtypes: neutrophils, plasmacytoid dendritic cells (pDCs), natural killer (NK)T cells ($CD56^+/CD16^+$), monocytes ($CD14^{high}$) and $CD8^+$ T cells ($PD\text{-}1^+$). This signature achieved a high accuracy (C-index 0.74 vs 0.71) for predicting OS benefit in the training and validation cohort. Both in the training and validation cohort, the low-risk group had significantly longer OS than the high-risk group (HR 0.26, 95% CI: 0.12-0.56, p=0.00025; HR 0.30, 95% CI: 0.10 -0.91, p=0.024, respectively). In the whole cohort, FCBPS is a predictor of OS (HR_{OS}=0.28, 95% CI: 0.15-0.52) and progression-free survival (HR_{PFS}=0.22, 95% CI: 0.12-0.39) that remained independent in multivariate analyses and subgroup analyses after adjusting for clinical and pathological factors. The identified flow cytometry-based whole-blood prognostic signature (FCBPS) is a powerful predictor for metastatic cancer patients who benefit from ICI treatment.

Keywords: immune checkpoint inhibitors, solid cancers, flow cytometry, peripheral blood immunophenotyping, prognostic signature

Trial registration: Prospectively registered in ClinicalTrials.gov (NCT03453892) on January 24, 2018.

Introduction

Immune checkpoint inhibitors (ICI) can effectively restore the activity of exhausted CD8 positive cytotoxic T cells and thereby trigger efficient anti-tumor immune responses. During the last years, several ICI were approved for more than ten different tumor entities. However, only some patients show durable responses, whereas the majority still does not benefit from this kind of immune therapy [1]. In clinical trials the expression of programmed cell death-ligand 1 (PD-L1) on tumor and/or immune cells has been frequently used to select patient subgroups with higher chances of treatment response. However, the predictive power of PD-L1 expression is not satisfactory [2, 3]. Furthermore, PD-L1 is no stable marker as it increases e.g. after radiotherapy [4, 5]. Consequently, large effort has been made to identify better predictive and prognostic markers for treatment responses to ICI, such as genomic instability [6]. The latter has been assessed via tumor mutational burden (TMB) [7] or mismatch repair deficiency [8]. All of these methods predicted treatment response to a certain extent, but were not precise enough to be used in clinical routine. A further challenge is imaging of the treatment response. Tumor lesions treated with ICI can increase in size during the first weeks of treatment due to inflammation [9]. This pseudoprogression cannot easily be distinguished from an increase in size due to tumor growth. Consequently, the classical RECIST 1.1 criterial were modified to the iRECIST criteria, which recommend treatment beyond the first progression [10]. The main problem of this procedure is that patients with real tumor progression loose time for a probably more efficient chemotherapy.

A recent strategy to complement these approaches is to analyze changes of peripheral blood immune cells at early time points during treatment. The peripheral blood immune status may have a predictive power for treatment response of solid tumors to ICI, as several immune cells that were already proven to predict treatment responses when being present in the tumor tissue also circulate through peripheral blood [11]. Furthermore, drawing of peripheral blood can be repeated easily and without an additional risk for the patients compared to repeated biopsies of the tumor tissue. Immunophenotyping of peripheral blood from patients with stage IV melanoma before and after treatment with ICI identified pharmacodynamic changes in circulating

CD8+ T cells with an exhausted-phenotype. Clinical failure of patients was identified to be associated with an imbalance between T-cell reinvigoration and tumor burden [12]. Another study identified a predictive character of proliferating (Ki-67+) PD1+CD8+ T cells for response to anti-PD-1 immunotherapy in solid tumors [13]. Using high-dimensional single-cell mass cytometry, Krieg and colleagues found HLA-DR high expressing monocytes to be of predictive value for responses to anti-PD-1 therapy [14]. In the ST-ICI trial, preplanned biomarker analysis was performed and the peripheral blood immune phenotype of patients treated with ICI was prospectively monitored by multi-color flow cytometry. A total of 54 immune cell types were analyzed. The aim of this study was to construct a signature, based on changes of the peripheral blood immunophenotype that identifies at an early time point of therapy patients who benefit from ICI.

Materials and Methods

Patients

Patients with clinically indicated treatment with ICI were eligible for this prospective non-interventional study. Patients could be included independent from cancer entity and concomitant radiotherapy. Criteria for eligibility were adult age of at least 18 years and the willingness of the patients to allow regular blood draws for immune phenotyping of peripheral blood. As the trial should represent the real life situation, there were no limitations regarding baseline Eastern Cooperative Oncology Group (ECOG) performance status or baseline routine blood parameters. Exclusion criteria were fertile patients who refused effective contraception during study treatment, persistent drug and/or alcohol abuse, patients not speaking German, patients in legal care and imprisoned patients.

Study design and treatments

Patients that were treated with ICI directed against programmed cell death protein 1 (PD-1) or PD-L1 were collected from the ST-ICI study (NCT03453892). All ICI were indicated by the treating physician according to current guidelines and clinical standards. The following ICI were used: Nivolumab (Opdivo, Bristol-Myers Squibb,

New York City, NY, USA), Pembrolizumab (Keytruda, Merck Sharp & Dohme, Kenilworth, NJ, USA), Atezolizumab (Tecentriq, Roche Co., Basel, Switzerland), Durvalumab (Imfinzi, AstraZeneca Group plc, Cambridge, England, U.K.), Avelumab (Bavencio, Pfizer and Merck KGaA, Darmstadt, Germany). Dosing of the ICI was according to the European Medicines Agency (EMA) marketing authorizations.

The institutional review board at the Friedrich-Alexander-Universität Erlangen-Nürnberg approved the study (number: 2_17 B). The study was performed in accordance with the Declaration of Helsinki. All patients gave written informed consent before enrollment that comprised a data privacy clause for data collection and analysis for research purpose. The research design for the identification of a prognostic signature for patients treated with ICI is displayed in Figure 1A. The redaction of the manuscript followed the STROBE guidelines for observational studies.

Endpoints and assessments

The primary endpoint of the here presented analyses was the association between changes of the patients' peripheral blood immunophenotypes and the clinical outcomes. Main clinical outcome parameters were overall survival (OS), progression free survival (PFS) and treatment response. OS and PFS were calculated beginning from the first administration of the ICI. Peripheral whole blood immune phenotyping was performed before each administration of the ICI. The current analysis included the early immune phenotypes, namely before the second administration of the ICI.

Multi-colour flow cytometry

Whole blood samples were collected and analyzed by multi-colour flow cytometry according to our previously published modularly immunophenotyping (IPT) protocols [15, 16]. IPT was performed within three hours after the collection of whole blood in order to determine a detailed immune status. Data acquisition was performed on a Gallios Flow Cytometer (Beckman Coulter) in the standard filter configuration. The Kaluza® Flow Analysis Software (Beckman Coulter) was used for data analysis. The immune cell subsets which were analyzed are specified in sFigure 1.

Data collection

Differences in OS were analysed in dependence of absolute immune cell counts of each subset and in dependence of clinical factors (gender, age, the presence of brain metastases, types of tumour, PD-L1 expression).

Development and validation of the flow cytometry-based whole-blood prognostic signature (FCBPS)

The overall workflow of this study is displayed in Figure 1B. Univariate Cox proportional hazard regression was applied to examine the association between peripheral blood immunophenotypes and patients' OS [17]. Peripheral blood immune cells statistically significant associated ($P < 0.2$) with OS of the patients served as candidates for further analyses. To uncover the practicability and accuracy of FCBPS for patients treated with ICI, all patients were divided randomly into the training (70%) and validation (30%) cohorts. Least absolute shrinkage and selection operator (LASSO) could reduce the complexity of the model and can well be used with the Cox proportional hazard regression model for survival analysis with high dimensional data [18, 19]. The Cox-LASSO regression model was administered to develop a multi-immunophenotype-based prognostic signature for OS prediction in the training cohort. After 200,000-time steps for LASSO, the best c-index related model was selected as FCBPS. Subsequently, we analyzed data in a validation cohort for this model to assess its feasibility and reliability in patients treated with ICI. The optimal cut off value for the risk score was determined by *surv_cutpoint* function in *survminer* package. All patients were divided into different groups (high-risk or low-risk) based on the cut-off of the risk score, which was calculated by considering the expression of immunophenotypes and the correlation coefficient.

Statistical analysis

Associations between clinical characteristics in the training and the validation cohorts were evaluated using the chi-square test. OS time was defined from the date of the first administration of the ICI to the date of last follow-up or death. The Kaplan-Meier method and Cox proportional hazard regression models were applied to compare survival of different groups with immunophenotypes, FCBPS and related clinical factors. Univariate, multivariate and subgroup analyses were used to evaluate the

impact of other confounding factors. Results of Cox regression analysis are described by means of hazard ratios (HR), 95%CI of HR and *P* values (Wald test). The concordance index (C-index) and the time-dependent receiver operating characteristic (ROC) curve, and the area under the ROC curve (AUC) values were calculated for different models as a measure of the discriminatory ability that allows comparison of signatures. A signature with a c-index of 0.5 has no predictive value; a model with a c-index of 1 would allow a perfect prediction of the patient's outcome [20]. The C-index was analyzed using the *survcomp* (version 1.22.0) [21]. The ROC curve and AUC values were calculated with the *timeROC* package (version 0.3); for survival analyses the *survival* package was used. All of analyses were carried out using R version 3.6.1 (R Foundation for Statistical Computing) and related packages. $P \leq 0.05$ was considered to be statistically significant.

Results

Patient characteristics

A total of 104 patients were prospectively enrolled in the ST-ICI trial between April 2017 and August 2019 (Figure 1B). Whole blood samples for immunophenotyping before the second ICI administration were available of 89 patients. Patient characteristics are presented in Table 1. The median age was 65.8 years; 73% were male. Most frequent tumor entities were head and neck squamous cell carcinoma (HNSCC) in 40 patients (45%) and non-small cell lung cancer (NSCLC) in 39 patients (44%). The used drugs were Nivolumab in 58 patients (65%), Pembrolizumab in 20 patients (23%), Durvalumab in 8 patients (9%), Avelumab in 2 patients (2%), Atezolizumab in 1 patient (1%).

The ICI was first line treatment in 19 patients (21%) in the recurrent and/or metastatic setting, 13 patients (15%) had received one prior systemic treatment and 57 patients (64%) two or more prior systemic treatments. The median follow up was 8.3 months. A total of 57 OS-events and 72 PFS-events occurred during the follow up period. Median OS was 8.7 months, median PFS was 4.2 months.

Development and definition of the FCBPS

After data clean, 54 peripheral blood immune markers were included into an univariate cox survival analysis. The following 14 of them were associated with OS (P< 0.2): monocytes ($CD14^{high}$), monocytes ($CD14^{low}$), neutrophils, dendritic cells (DCs), myeloid (m)DCs-1, mDCs-2, plasmacytoid DCs (pDCs), natural killer (NK) cells ($CD56^{high}/CD16^{+}$), NKT cells ($CD56^{+}/CD16^{+}$), NKT cells ($CD16^{+}$), CD8+ T cells ($PD\text{-}1^{+}$), $CD8^{+}$ T cells ($CD25^{+}$), $CD8^{+}$ T cells ($CD69^{+}$), and regulatory T cells (Tregs) (Table 2).

Then the ST-ICI cohort was randomly assigned to a training cohort (n=56) and a validation cohort (n=33) for further LASSO proportional hazards Cox regression analysis. After 200,000 times repeat LASSO regression, the highest C-index's model was chosen as the FCBPS. This prognostic signature model obtained from the training cohort found the following risk score = (0.00001219963 × the absolute immune cell counts of neutrophils) + (-0.0335468 × the absolute immune cell counts of pDCs) + (-0.08766993 × the absolute immune cell counts of NKT cells ($CD56^{+}/CD16^{+}$)) +(-0.01120408 × the absolute immune cell counts of monocytes($CD14^{high}$)) + (0.004149556 × the absolute immune cell counts of $CD8^{+}$T cells ($PD\text{-}1^{+}$)). In this signature, neutrophils and $CD8^{+}$ T cells ($PD\text{-}1^{+}$) were positive coefficients, which means that patients with increasing absolute counts had a shorter OS. However, pDCs, NKT cells ($CD56^{+}/CD16^{+}$) and monocytes ($CD14^{high}$) were negative coefficients, which means that patients with increasing absolute cell counts had a longer OS.

According to best C-index (0.74, 96%CI 0.67-0.82), the optimal cut-off is -0.487, which classified the training cohort into a low- risk group (n=44) and a high-risk group (n=12) (Figure 2 A-C). In the training cohort, each unit increase in FCBPS was associated with a 0.26 fold increase in the rate of OS events (95%CI: 0.12-0.56, P =0.00025). Median OS in the FCBPS low- and high-risk groups was 14.5 (95% CI: 10.1-NE (not estimable)) vs 5.4 (95% CI: 3.0-NE) months, respectively (Figure 3A).

The validation cohort was classified using the same cut-off of FCBPS into a low-risk group (n=29) and a high-risk group (n=4) (Figure 2D-F). The validation cohort confirmed the proposed risk model (C-index=0.71, 95%CI: 0.62-0.81). The median

OS in the low- and high-risk groups was 11.5 (95% CI: 9.2- 20.6) vs 3.7 (95% CI: 2.8- NE) months (HR=0.30, 95% CI: 0.10–0.91, P = 0.024), respectively (Figure 3C).

The sensitivity and specificity of FCBPS for predicting the OS were plotted in a time-dependent ROC. In the training cohort, the AUC values for 6-, 12- and 24-month OS prediction were 0.811, 0.708 and 0.788 respectively (Figure 3B). In the validation cohort, the AUC values for 6-, 12- and 24-month OS prediction were 0.731, 0.716 and 0.768, respectively (Figure 3D). In the total ST-ICI cohort, median OS in the low- and high-risk groups was 12.5 (95% CI: 9.8-19.7) vs 4.7 (95% CI: 3.0- NE) months (HR=0.28, 95% CI: 0.15–0.52, P<0.001), respectively (Figure 4A). The time-ROC results indicate that this signature is still a powerful predictor for OS in the whole cohort (AUC_{6m}=0.77, AUC_{12m}=0.72, AUC_{6m}=0.82) (Figure 4B). At the same time, FCBPS also can predict progression-free survival benefit for patients treated with ICI (low-risk vs high-risk: HR=0.22 [95%CI 0.12-0.39]; the median PFS of low risk and high risk are 6.3 and 2.0 months, respectively (Figure 4C); AUC_{6m}=0.69, AUC_{12m}=0.68, AUC_{6m}=0.69 (Figure 4D)). These results indicate that the developed FCBPS can predict which cancer patients have prolonged OS and PFS after treatment with anti-PD-1 or anti-PD-L1.

Validation of the FCBPS as an independent prognostic signature

To determine whether the FCBPS could serve as an independent prognostic factor, Cox proportional hazard regression model was used for the detection of the relationships between OS and the clinical factors (Table 3). In the ST-ICI cohort, univariate analysis showed that FCBPS and brain metastasis were significantly associated with OS, while multivariate analysis showed that age, PD-L1 expression 50-100 % and FCBPS significantly associated with OS (P < 0.05). FCBPS and PD-L1 expression 1-49 % were significantly associated with PFS in univariate and multivariate analysis. These results indicate that FCBPS remained an independent survival benefit predictor for advanced cancer patients treated with ICI.

Subgroup Analyses

Post-hoc subgroup analyses based on patient characteristics suggested that OS and PFS hazard ratios favoured the FCBPS low risk group in most subgroups (Figure 5,

sFigure 2-6). Regarding OS, the subgroup analyses by PD-L1 expression suggested that median OS tended to be longer in patients with PD-L1 expression < 1% in the low-risk group (HR= 0.45 (95%CI 0.16-1.24), 9.1 months [95% CI 4.5–21] vs 5.0 months [3.0–NE]; Figure 5A, sFigure 3). However, no differences of OS and PFS were found between low-risk and high-risk groups in patients with brain metastasis (sFigure 4). Median OS and PFS of patients stratified by age, gender, and tumour entity are shown in the sFigures.

Discussion

In recent years, ICI with or without chemotherapy were approved for different recurrent or metastatic cancers. However, only around 20% of non-selected patients experience long-term benefit [2, 22]. Numerous studies suggest that TMB may predict clinical response to ICI [23-25]. However, different studies used different cut-off values to define low and high TMB. The detection of PD-L1 by different methods or cut-off values could also guide anti-PD-1/PD-L1 therapy, but still harbours the risk of a false-negative patient stratification [26-28]. The gene methylation status may also serve to select patients who will experience clinical benefit from PD-1 blockade [29].There is still need of new and/or complementary timesaving, cost-effective, safe and easy applicable tools to identify cancer patients who should benefit from ICI.

In this context, a detailed knowledge about immunity, both in the tumor microenvironment and in the periphery, is needed to judge about the potential of cancer immunotherapy and the efficacies of immunotherapies [30]. Tumor immunogenicity scores are under evaluation as predictors for responses to ICI [31]. Previous studies already indicated peripheral blood immune cell subsets like PD-1^{+}CD56^{+} T cells [32] or CD4+ and CD8+ cells [33] to be associated with favourable outcome for advanced melanoma patients treated with ipilimumab directed against cytotoxic T lymphocyte antigen-4 (CTLA-4). Now we identified a flow cytometry-based whole-blood prognostic immune signature to early identify patients who benefit from anti-PD-1/PD-L1 treatment.

To our best knowledge, the ST-ICI trial is the first prospective study that prospectively

included a whole-blood flow cytometry-based approach in a multi-type advanced cancer patient cohort treated with anti-PD-1/PD-L1 ICI. Before, most of the studies focused on the analyses of peripheral blood mononuclear cells (PBMCs) to detect possible immune biomarkers. However, the conventional PBMCs assays require a large volume of blood and are more cost intensive compared to whole blood assays and do exclude granulocytes from the analyses. Thus, whole blood assays gain importance in easy screening of larger numbers of blood parameters; in the analyses within the ST-ICI trial, 54 immune cell subsets were monitored with the need of less than 1 ml of peripheral whole blood. In a first step, 14 immune cell subsets were identified to be associated with OS. Furthermore, LASSO regression constructed the FCBPS signature including neutrophils, pDCs, NKT cells ($CD56^{+}/CD16^{+}$), monocytes($CD14^{high}$) and $CD8^{+}$T cells ($PD\text{-}1^{+}$). This signature includes innate and adaptive immune cells and serves as an effective tool for the identification of patients who benefit from ICI treatment. It is becoming more and more evident that multiple immune cell subsets in a concerted action may help for selecting patients that are likely to respond to ICI [34].

We identified that increasing amounts of neutrophils in the peripheral blood of cancer patients were associated with less benefit from ICI treatment. Neutrophils were reported to support e.g. the development of metastasis through multiple mechanisms, such as the release of proteases that degrade antitumor factors, and leukotrienes that propagate metastasis-initiating cells. In addition, pro-tumorigenic neutrophils suppress antitumor T cell responses [35]. Decreased migration of neutrophils to tumor areas or the inhibition of granulocyte colony stimulating factor to decrease the amount of neutrophils has already shown efficacy in preclinical models [36]. Regarding innate immune cells not of the granulocytic, but of the monocytic compartment, increased amounts of CD14 high expressing monocytes in the peripheral blood correlated with improved prognosis. This is in accordance with the findings of Krieg et al [37] who identified CD14+/HLA-DR+ monocytes as a strong predictor of PFS and OS in response to anti-PD-1 immunotherapy in melanoma patients.

Further, we found that increased amounts of plasmacytoid dendritic cells (pDCs) are beneficial for the PFS and OS. pDCs have a central role in activating host innate and adaptive immune responses and they are known as the major IFN type I-producing cells. Thereby, pDCs activate many other cell types, such as monocytes, NK cells, and T cells which are known to be also central for anti-tumor immune responses [38]. High levels of circulating pDCs were found to be predict a favorable outcome in patients with breast cancer [39] and for patients with pancreatic adenocarcinoma [40].

NKT cells are suggested to induce a cross talk of pDCs with conventional DCs that result in induction of memory CD8+ T cells [41]. We identified increased numbers of NKT cells in patients of the ST-ICI trial to be favorable for PFS and OS. Just recently, it was shown for patients with NSCLC that increased amounts of peripheral NK cells correlate with responses to anti-PD-1 treatment [42]. The role for NKT cells in this scenario has not been investigated before, but it is becoming more and more evident that NKT cells are important in anti-tumor immunity as they e.g. reinvigorate exhausted immune cells in the tumor microenvironment [43].

Exhausted immune cells fail to contribute to anti-tumor immunity. Increased numbers of PD-L1+ NK cells in the peripheral blood, e.g., are associated with poor response to anti-PD-1 treatment of patients with NSCLC [44]. However, intratumoral $CD8^+$ T cells which are positive for $PD\text{-}1^+$ were shown to be predictive for response and survival upon anti-PD-1 treatment, as shown in a small cohort of patients with NSCLC [45]. Studies in chronic myeloid leukemia patients just recently revealed that differences in PD-1 Expression on CD8+ T-cells may predict the disease course [46]. Our immune monitoring suggests that increased amounts of circulating PD-1+ $CD8^+$ T cells at early time points of ICI therapy predict a poorer OS and PFS in patients with solid tumors treated with ICI. This might indicate that in these cases the activated CD8+ T cells cannot enter properly into the tumor and exert their anti-tumor activity.

The ST-ICI cohort composes a “real-life” cohort, which goes along with some confounding factors like treatment with different ICI, different tumor types, brain metastasis, and PD-L1 expression. However, the multivariable Cox regression and

subgroup analyses suggests that FCBPS is an independent prognostic factor for advanced cancer patients treated with ICI. Subgroup analysis suggest that this immune signature can stably predict OS and PFS benefit for cancer patients treated with ICI in any subgroups, except for brain metastasis. Although patients with brain metastases can benefit from ICI treatment [47], the knowledge about the immune microenvironment at this tumor location side is still scarce [48, 49], and future trials will have to particularly focus on this subgroup of the ST-ICI study population. In present clinical practices, PD-L1 expression is an essential biomarker as drug approvals depend on its expression. However, our subgroup analyses revealed that the FCBPS predicts survival benefits independent from the PD-L1 expression status. FCBPS identified more than 82% of all advanced cancer patients, who benefit fromanti-PD-1/PD-L1 treatments.

Conclusion

This prospective study demonstrated that FCBPS could predict at a very early time point of immune therapy which cancer patients with advanced disease will benefit from ICI treatment and therefore could guide clinical decisions in the future. This newly identified FCBPS is a low-cost, safe, easy applicable and effective predictor for OS and PFS in cancer patients treated with ICI.

Availability of data and materials

The datasets used and/or analyzed during the current study are available from the corresponding author on reasonable request.

Acknowledgements

The authors thank the patients who participated in the study, their supporters, the investigators, and clinical research staff from the Department of Radiation Oncology. We thank Dr. Bailiang Li from Stanford University School of Medicine for share the code for RMS plot. The present work was performed by Jian-Guo Zhou in (partial) fulfilment of the requirements for containing the degree “Dr. rer. biol. hum”.

Funding

There was no external funding for this trial. The study was supported by the Department of Radiation Oncology, Universitätsklinikum Erlangen, Friedrich-Alexander-Universität Erlangen-Nürnberg, Erlangen, Germany and partly supported by the BMBF (GREWIS-alpha, 02NUK050E).

Contributions

Conception and design: MH, USG, BF, RF, HM, JGZ, ME, AD

Development of methodology: JGZ, AD

Acquisition of data: AD, SR, IB, BF, ME, MH, USG

Analysis and interpretation of data: JGZ, AD, ED, RS, PS, USG, MH

Writing, review, and/or revision of the manuscript: JGZ, AD, RF, MH, USG, ED, RS, CS, PS

Administrative, technical, or material support: SR, CS, MH

Study supervision: USG, MH, RF, BF

Ethics approval and consent to participate

The protocol, any amendments, and informed consent forms were approved by the institutional review boards/independent ethics committees (number: 2_17 B). The study was performed in accordance with the Declaration of Helsinki. All patients gave written informed consent before enrolment that comprised a data privacy clause for data collection and analysis for research purpose.

Competing interests

MH reports conflict of interest with Merck Serono (advisory boards, honoraria for lectures, travel grants, research funding); MSD (advisory boards, travel grants, research funding); AstraZeneca (research funding); Novartis (research funding); BMS (advisory boards, honoraria for lectures); Teva (travel grants). USG received support for presentation activities for Dr. Sennewald Medizintechnik GmbH, has received support for investigator initiated clinical studies (IITs) from MSD and AstraZeneca and

contributed at Advisory Boards Meetings of AstraZeneca and Bristol-Myers Squibb. JGZ received support from AstraZeneca (travel grants). HM reports conflict of interest with Merck Serono (advisory boards, honoraria for lectures, travel grants); MSD (advisory boards, honoraria for lectures, travel grants); AstraZeneca (advisory boards, honoraria for lectures, travel grants); BMS (advisory boards, honoraria for lectures, travel grants). RS received travel and accommodation expenses from AstraZeneca. ED reports grants and honoraria from ROCHE GENENTECH, grants from SERVIER, grants and honoraria from ASTRAZENECA, MERCK SERONO, BMS and MSD, outside the submitted work. SR conflict of interest with AstraZeneca (research funding); MSD (research funding). ME conflict of interest with Diaceutics (employment, honoraria, advisory role, speakers' bureau, travel expenses); AstraZeneca (honoraria, advisory role, speakers' bureau, travel expenses); Roche (honoraria, travel expenses); MSD (honoraria, speakers' bureau); GenomicHealth (honoraria, advisory role, speakers bureau, travel expenses); Astellas (honoraria, speakers' bureau); Janssen-Cilag (honoraria, advisory role, research funding, travel expenses); Stratifyer (research funding, patents). RF conflict of interest with MSD (honoraria, advisory role, research funding, travel expenses); Fresenius (honoraria); BrainLab (honoraria); AstraZeneca (honoraria, advisory role, research funding, travel expenses); Merck Serono (advisory role, research funding, travel expenses); Novocure (advisory role, speakers' bureau, research funding); Sennewald (speakers' bureau, travel expenses).

References

[1] S. Das, D.B. Johnson, Immune-related adverse events and anti-tumor efficacy of immune checkpoint inhibitors, Journal for ImmunoTherapy of Cancer, 7 (2019) 306.

[2] B. Burtness, K.J. Harrington, R. Greil, D. Soulières, M. Tahara, G.D. Castro, A. Psyrri, N. Baste Rotllan, P.C. Neupane, A. Bratland, T. Fuereder, B.G.M. Hughes, R. Mesia, N. Ngamphaiboon, T. Rordorf, W.Z. Wan Ishak, A. Roy, J. Cheng, F. Jin, D. Rischin, KEYNOTE-048: Phase III study of first-line pembrolizumab (P) for recurrent/metastatic head and neck squamous cell carcinoma (R/M HNSCC), Annals of Oncology, 29 (suppl_8) (2018).

[3] T.S.K. Mok, Y.L. Wu, I. Kudaba, D.M. Kowalski, B.C. Cho, H.Z. Turna, G. Castro, Jr., V. Srimuninnimit, K.K. Laktionov, I. Bondarenko, K. Kubota, G.M. Lubiniecki, J. Zhang, D. Kush, G. Lopes, K.-. Investigators, Pembrolizumab versus chemotherapy for previously untreated, PD-L1-expressing, locally advanced or metastatic non-small-cell lung cancer (KEYNOTE-042): a randomised, open-label, controlled, phase 3 trial, Lancet, 393 (2019) 1819-1830.

[4] M. Hecht, M. Buttner-Herold, K. Erlenbach-Wunsch, M. Haderlein, R. Croner, R. Grutzmann, A. Hartmann, R. Fietkau, L.V. Distel, PD-L1 is upregulated by radiochemotherapy in rectal adenocarcinoma patients and associated with a favourable prognosis, European journal of cancer, 65 (2016) 52-60.

[5] A. Derer, M. Spiljar, M. Bäumler, M. Hecht, R. Fietkau, B. Frey, U.S. Gaipl, Chemoradiation Increases PD-L1 Expression in Certain Melanoma and Glioblastoma Cells, Front Immunol, 2016, pp. 610.

[6] J.M. Zaretsky, A. Garcia-Diaz, D.S. Shin, H. Escuin-Ordinas, W. Hugo, S. Hu-Lieskovan, D.Y. Torrejon, G. Abril-Rodriguez, S. Sandoval, L. Barthly, J. Saco, B. Homet Moreno, R. Mezzadra, B. Chmielowski, K. Ruchalski, I.P. Shintaku, P.J. Sanchez, C. Puig-Saus, G. Cherry, E. Seja, X. Kong, J. Pang, B. Berent-Maoz, B. Comin-Anduix, T.G. Graeber, P.C. Tumeh, T.N. Schumacher, R.S. Lo, A. Ribas, Mutations Associated with Acquired Resistance to PD-1 Blockade in Melanoma, N Engl J Med, 375 (2016) 819-829.

[7] N.I. Vokes, D. Liu, B. Ricciuti, E. Jimenez-Aguilar, H. Rizvi, F. Dietlein, M.X. He, C.A. Margolis, H.A. Elmarakeby, J. Girshman, A. Adeni, F. Sanchez-Vega, N. Schultz, S. Dahlberg, A. Zehir, P.A. Janne, M. Nishino, R. Umeton, L.M. Sholl, E.M. Van Allen, M.D. Hellmann, M.M. Awad, Harmonization of Tumor Mutational Burden Quantification and Association With Response to Immune Checkpoint Blockade in Non-Small-Cell Lung Cancer, JCO Precis Oncol, 3 (2019).

[8] D.T. Le, J.N. Uram, H. Wang, B.R. Bartlett, H. Kemberling, A.D. Eyring, A.D. Skora, B.S. Luber, N.S. Azad, D. Laheru, B. Biedrzycki, R.C. Donehower, A. Zaheer, G.A. Fisher, T.S. Crocenzi, J.J. Lee, S.M. Duffy, R.M. Goldberg, A. de la Chapelle, M. Koshiji, F. Bhaijee, T. Huebner, R.H. Hruban, L.D. Wood, N. Cuka, D.M. Pardoll, N. Papadopoulos, K.W. Kinzler, S. Zhou, T.C. Cornish, J.M. Taube, R.A. Anders, J.R. Eshleman, B. Vogelstein, L.A. Diaz, Jr., PD-1 Blockade in Tumors with Mismatch-Repair Deficiency, N Engl J Med, 372 (2015) 2509-2520.

[9] L.F. Chai, E. Prince, V.G. Pillarisetty, S.C. Katz, Challenges in assessing solid tumor responses to immunotherapy, Cancer Gene Ther, (2019).
[10] L. Seymour, J. Bogaerts, A. Perrone, R. Ford, L.H. Schwartz, S. Mandrekar, N.U. Lin, S. Litiere, J. Dancey, A. Chen, F.S. Hodi, P. Therasse, O.S. Hoekstra, L.K. Shankar, J.D. Wolchok, M. Ballinger, C. Caramella, E.G. de Vries, R.w. group, iRECIST: guidelines for response criteria for use in trials testing immunotherapeutics, Lancet Oncol, 18 (2017) e143-e152.
[11] J.A. Chen, W. Ma, J. Yuan, T. Li, Translational Biomarkers and Rationale Strategies to Overcome Resistance to Immune Checkpoint Inhibitors in Solid Tumors, Cancer treatment and research, 180 (2020) 251-279.
[12] A.C. Huang, M.A. Postow, R.J. Orlowski, R. Mick, B. Bengsch, S. Manne, W. Xu, S. Harmon, J.R. Giles, B. Wenz, M. Adamow, D. Kuk, K.S. Panageas, C. Carrera, P. Wong, F. Quagliarello, B. Wubbenhorst, K. D'Andrea, K.E. Pauken, R.S. Herati, R.P. Staupe, J.M. Schenkel, S. McGettigan, S. Kothari, S.M. George, R.H. Vonderheide, R.K. Amaravadi, G.C. Karakousis, L.M. Schuchter, X. Xu, K.L. Nathanson, J.D. Wolchok, T.C. Gangadhar, E.J. Wherry, T-cell invigoration to tumour burden ratio associated with anti-PD-1 response, Nature, 545 (2017) 60-65.
[13] K.H. Kim, J. Cho, B.M. Ku, J. Koh, J.M. Sun, S.H. Lee, J.S. Ahn, J. Cheon, Y.J. Min, S.H. Park, K. Park, M.J. Ahn, E.C. Shin, The First-week Proliferative Response of Peripheral Blood PD-1(+)CD8(+) T Cells Predicts the Response to Anti-PD-1 Therapy in Solid Tumors, Clin Cancer Res, 25 (2019) 2144-2154.
[14] C. Krieg, M. Nowicka, S. Guglietta, S. Schindler, F.J. Hartmann, L.M. Weber, R. Dummer, M.D. Robinson, M.P. Levesque, B. Becher, High-dimensional single-cell analysis predicts response to anti-PD-1 immunotherapy, Nat Med, 24 (2018) 144-153.
[15] P.F. Rühle, R. Fietkau, U.S. Gaipl, B. Frey, Development of a Modular Assay for Detailed Immunophenotyping of Peripheral Human Whole Blood Samples by Multicolor Flow Cytometry, Int J Mol Sci, 17 (2016) 1316.
[16] A.-J. Donaubauer, P.F. Rühle, I. Becker, R. Fietkau, U.S. Gaipl, B. Frey, One-Tube Multicolor Flow Cytometry Assay (OTMA) for Comprehensive Immunophenotyping of Peripheral Blood, in: M. Steinitz (Ed.) Human Monoclonal Antibodies: Methods and Protocols, Springer New York, New York, NY, 2019, pp. 189-212.
[17] N. Simon, J. Friedman, T. Hastie, R. Tibshirani, Regularization Paths for Cox's Proportional Hazards Model via Coordinate Descent, J Stat Softw, 39 (2011) 1-13.
[18] J.-G. Zhou, H.-T. Zhao, S.-H. Jin, X. Tian, H. Ma, Identification of a RNA-seq-based signature to improve prognostics for uterine sarcoma, Gynecologic Oncology, 155 (2019) 499-507.
[19] J.-G. Zhou, B. Liang, S.-H. Jin, H.-L. Liao, G.-B. Du, L. Cheng, H. Ma, U.S. Gaipl, Development and Validation of an RNA-Seq-Based Prognostic Signature in Neuroblastoma, Frontiers in Oncology, 9 (2019).
[20] A.R. Brentnall, J. Cuzick, Use of the concordance index for predictors of censored survival data, Stat Methods Med Res, 27 (2018) 2359-2373.
[21] B. Haibe-Kains, C. Desmedt, C. Sotiriou, G. Bontempi, A comparative study of survival models for breast cancer prognostication based on microarray data: does a

single gene beat them all?, Bioinformatics, 24 (2008) 2200-2208.
[22] R.S. Herbst, P. Baas, D.W. Kim, E. Felip, J.L. Perez-Gracia, J.Y. Han, J. Molina, J.H. Kim, C.D. Arvis, M.J. Ahn, M. Majem, M.J. Fidler, G. de Castro, Jr., M. Garrido, G.M. Lubiniecki, Y. Shentu, E. Im, M. Dolled-Filhart, E.B. Garon, Pembrolizumab versus docetaxel for previously treated, PD-L1-positive, advanced non-small-cell lung cancer (KEYNOTE-010): a randomised controlled trial, Lancet, 387 (2016) 1540-1550.
[23] Z. Wang, J. Duan, S. Cai, M. Han, H. Dong, J. Zhao, B. Zhu, S. Wang, M. Zhuo, J. Sun, Q. Wang, H. Bai, J. Han, Y. Tian, J. Lu, T. Xu, X. Zhao, G. Wang, X. Cao, F. Li, D. Wang, Y. Chen, Y. Bai, J. Zhao, Z. Zhao, Y. Zhang, L. Xiong, J. He, S. Gao, J. Wang, Assessment of Blood Tumor Mutational Burden as a Potential Biomarker for Immunotherapy in Patients With Non-Small Cell Lung Cancer With Use of a Next-Generation Sequencing Cancer Gene Panel, JAMA oncology, 5 (2019) 696-702.
[24] R.M. Samstein, C.-H. Lee, A.N. Shoushtari, M.D. Hellmann, R. Shen, Y.Y. Janjigian, D.A. Barron, A. Zehir, E.J. Jordan, A. Omuro, T.J. Kaley, S.M. Kendall, R.J. Motzer, A.A. Hakimi, M.H. Voss, P. Russo, J. Rosenberg, G. Iyer, B.H. Bochner, D.F. Bajorin, H.A. Al-Ahmadie, J.E. Chaft, C.M. Rudin, G.J. Riely, S. Baxi, A.L. Ho, R.J. Wong, D.G. Pfister, J.D. Wolchok, C.A. Barker, P.H. Gutin, C.W. Brennan, V. Tabar, I.K. Mellinghoff, L.M. DeAngelis, C.E. Ariyan, N. Lee, W.D. Tap, M.M. Gounder, S.P. D'Angelo, L. Saltz, Z.K. Stadler, H.I. Scher, J. Baselga, P. Razavi, C.A. Klebanoff, R. Yaeger, N.H. Segal, G.Y. Ku, R.P. DeMatteo, M. Ladanyi, N.A. Rizvi, M.F. Berger, N. Riaz, D.B. Solit, T.A. Chan, L.G.T. Morris, Tumor mutational load predicts survival after immunotherapy across multiple cancer types, Nature Genetics, 51 (2019) 202-206.
[25] M.D. Hellmann, T. Nathanson, H. Rizvi, B.C. Creelan, F. Sanchez-Vega, A. Ahuja, A. Ni, J.B. Novik, L.M.B. Mangarin, M. Abu-Akeel, C. Liu, J.L. Sauter, N. Rekhtman, E. Chang, M.K. Callahan, J.E. Chaft, M.H. Voss, M. Tenet, X.-M. Li, K. Covello, A. Renninger, P. Vitazka, W.J. Geese, H. Borghaei, C.M. Rudin, S.J. Antonia, C. Swanton, J. Hammerbacher, T. Merghoub, N. McGranahan, A. Snyder, J.D. Wolchok, Genomic Features of Response to Combination Immunotherapy in Patients with Advanced Non-Small-Cell Lung Cancer, Cancer Cell, 33 (2018) 843-852.e844.
[26] K. Takada, G. Toyokawa, T. Okamoto, M. Shimokawa, Y. Kozuma, T. Matsubara, N. Haratake, T. Akamine, S. Takamori, M. Katsura, F. Shoji, Y. Oda, Y. Maehara, A Comprehensive Analysis of Programmed Cell Death Ligand-1 Expression With the Clone SP142 Antibody in Non-Small-Cell Lung Cancer Patients, Clin Lung Cancer, 18 (2017) 572-582 e571.
[27] H.H. Lee, Y.N. Wang, W. Xia, C.H. Chen, K.M. Rau, L. Ye, Y. Wei, C.K. Chou, S.C. Wang, M. Yan, C.Y. Tu, T.C. Hsia, S.F. Chiang, K.S.C. Chao, Wistuba, II, J.L. Hsu, G.N. Hortobagyi, M.C. Hung, Removal of N-Linked Glycosylation Enhances PD-L1 Detection and Predicts Anti-PD-1/PD-L1 Therapeutic Efficacy, Cancer Cell, 36 (2019) 168-178 e164.
[28] Y. Okuma, H. Wakui, H. Utsumi, Y. Sagawa, Y. Hosomi, K. Kuwano, S. Homma, Soluble Programmed Cell Death Ligand 1 as a Novel Biomarker for Nivolumab Therapy for Non-Small-cell Lung Cancer, Clin Lung Cancer, 19 (2018) 410-417 e411.

[29] M. Duruisseaux, A. Martinez-Cardus, M.E. Calleja-Cervantes, S. Moran, M. Castro de Moura, V. Davalos, D. Pineyro, M. Sanchez-Cespedes, N. Girard, M. Brevet, E. Giroux-Leprieur, C. Dumenil, M. Pradotto, P. Bironzo, E. Capelletto, S. Novello, A. Cortot, M.C. Copin, N. Karachaliou, M. Gonzalez-Cao, S. Peralta, L.M. Montuenga, I. Gil-Bazo, I. Baraibar, M.D. Lozano, M. Varela, J.C. Ruffinelli, R. Palmero, E. Nadal, T. Moran, L. Perez, I. Ramos, Q. Xiao, A.F. Fernandez, M.F. Fraga, M. Gut, I. Gut, C. Teixido, N. Vilarino, A. Prat, N. Reguart, A. Benito, P. Garrido, I. Barragan, J.F. Emile, R. Rosell, E. Brambilla, M. Esteller, Epigenetic prediction of response to anti-PD-1 treatment in non-small-cell lung cancer: a multicentre, retrospective analysis, Lancet Respir Med, 6 (2018) 771-781.
[30] S. Gnjatic, V. Bronte, L.R. Brunet, M.O. Butler, M.L. Disis, J. Galon, L.G. Hakansson, B.A. Hanks, V. Karanikas, S.N. Khleif, J.M. Kirkwood, L.D. Miller, D.J. Schendel, I. Tanneau, J.M. Wigginton, L.H. Butterfield, Identifying baseline immune-related biomarkers to predict clinical outcome of immunotherapy, J Immunother Cancer, 5 (2017) 44.
[31] S. Wang, Z. He, X. Wang, H. Li, X.S. Liu, Antigen presentation and tumor immunogenicity in cancer immunotherapy response prediction, Elife, 8 (2019).
[32] J. Bochem, H. Zelba, T. Amaral, J. Spreuer, D. Soffel, T. Eigentler, N.B. Wagner, U. Uslu, P. Terheyden, F. Meier, C. Garbe, G. Pawelec, B. Weide, K. Wistuba-Hamprecht, Peripheral PD-1+CD56+ T-cell frequencies correlate with outcome in stage IV melanoma under PD-1 blockade, PLoS One, 14 (2019) e0221301.
[33] A. Martens, K. Wistuba-Hamprecht, J. Yuan, M.A. Postow, P. Wong, M. Capone, G. Madonna, A. Khammari, B. Schilling, A. Sucker, D. Schadendorf, P. Martus, B. Dreno, P.A. Ascierto, J.D. Wolchok, G. Pawelec, C. Garbe, B. Weide, Increases in Absolute Lymphocytes and Circulating CD4+ and CD8+ T Cells Are Associated with Positive Clinical Outcome of Melanoma Patients Treated with Ipilimumab, Clinical Cancer Research, 22 (2016) 4848-4858.
[34] F. Petitprez, M. Meylan, A. de Reyniès, C. Sautès-Fridman, W.H. Fridman, The Tumor Microenvironment in the Response to Immune Checkpoint Blockade Therapies, Front Immunol, 11 (2020) 784.
[35] T. Tüting, K.E.d. Visser, How neutrophils promote metastasis, Science, 352 (2016) 145-146.
[36] A. Ocana, C. Nieto-Jiménez, A. Pandiella, A.J. Templeton, Neutrophils in cancer: prognostic role and therapeutic strategies, Molecular Cancer, 16 (2017) 137.
[37] C. Krieg, M. Nowicka, S. Guglietta, S. Schindler, F.J. Hartmann, L.M. Weber, R. Dummer, M.D. Robinson, M.P. Levesque, B. Becher, High-dimensional single-cell analysis predicts response to anti-PD-1 immunotherapy, Nature Medicine, 24 (2018) 144-153.
[38] V. Koucký, J. Bouček, A. Fialová, Immunology of Plasmacytoid Dendritic Cells in Solid Tumors: A Brief Review, Cancers (Basel), 11 (2019) 470.
[39] J. Kini Bailur, B. Gueckel, G. Pawelec, Prognostic impact of high levels of circulating plasmacytoid dendritic cells in breast cancer, Journal of Translational Medicine, 14 (2016) 151.

[40] V. Tjomsland, P. Sandström, A. Spångeus, D. Messmer, J. Emilsson, U. Falkmer, S. Falkmer, K.-E. Magnusson, K. Borch, M. Larsson, Pancreatic adenocarcinoma exerts systemic effects on the peripheral blood myeloid and plasmacytoid dendritic cells: an indicator of disease severity?, BMC Cancer, 10 (2010) 87.
[41] K. Shimizu, M. Asakura, J. Shinga, Y. Sato, S. Kitahara, K. Hoshino, T. Kaisho, S.P. Schoenberger, T. Ezaki, S.-i. Fujii, Invariant NKT cells induce plasmacytoid dendritic cell (DC) cross-talk with conventional DCs for efficient memory CD8+ T cell induction, J Immunol, 190 (2013) 5609-5619.
[42] J.I. Youn, S.M. Park, S. Park, G. Kim, H.J. Lee, J. Son, M.H. Hong, A. Ghaderpour, B. Baik, J. Islam, J.W. Choi, E.Y. Lee, H.R. Kim, S.U. Seo, S. Paik, H.I. Yoon, I. Jung, C.F. Xin, H.T. Jin, B.C. Cho, S.Y. Seong, S.J. Ha, H.R. Kim, Peripheral natural killer cells and myeloid-derived suppressor cells correlate with anti-PD-1 responses in non-small cell lung cancer, Scientific reports, 10 (2020) 9050.
[43] E.A. Bae, H. Seo, I.K. Kim, I. Jeon, C.Y. Kang, Roles of NKT cells in cancer immunotherapy, Archives of pharmacal research, 42 (2019) 543-548.
[44] E.P. Juliá, P. Mandó, M.M. Rizzo, G.R. Cueto, F. Tsou, R. Luca, C. Pupareli, A.I. Bravo, W. Astorino, J. Mordoh, C. Martín, E.M. Levy, Peripheral changes in immune cell populations and soluble mediators after anti-PD-1 therapy in non-small cell lung cancer and renal cell carcinoma patients, Cancer immunology, immunotherapy : CII, 68 (2019) 1585-1596.
[45] D.S. Thommen, V.H. Koelzer, P. Herzig, A. Roller, M. Trefny, S. Dimeloe, A. Kiialainen, J. Hanhart, C. Schill, C. Hess, S. Savic Prince, M. Wiese, D. Lardinois, P.C. Ho, C. Klein, V. Karanikas, K.D. Mertz, T.N. Schumacher, A. Zippelius, A transcriptionally and functionally distinct PD-1(+) CD8(+) T cell pool with predictive potential in non-small-cell lung cancer treated with PD-1 blockade, Nat Med, 24 (2018) 994-1004.
[46] M.Y. Lee, C.J. Park, Y.U. Cho, E. You, S. Jang, C.A. Seol, E.J. Seo, E.J. Choi, J.H. Lee, Differences in PD-1 expression on CD8+ T-cells in chronic myeloid leukemia patients according to disease phase and TKI medication, Cancer immunology, immunotherapy : CII, (2020).
[47] A.M. Di Giacomo, M. Valente, A. Cerase, M.F. Lofiego, F. Piazzini, L. Calabrò, E. Gambale, A. Covre, M. Maio, Immunotherapy of brain metastases: breaking a “dogma”, Journal of Experimental & Clinical Cancer Research, 38 (2019) 419.
[48] H. Schmidberger, M. Rapp, A. Ebersberger, S. Hey-Koch, C.Loquai, S. Grabbe, A. Mayer, Long-term survival of patients after ipilimumab and hypofractionated brain radiotherapy for brain metastases of malignant melanoma: sequence matters, Strahlenther Onkol, 194 (2018) 1144-1151.
[49] M. Kocher, M. I. Ruge, N. Galldik, P. Lohmann, Applications of radiomics and machine learning for radiotherapy of malignant brain tumors, Strahlenther Onkol, (2020) May 11. doi: 10.1007/s00066-020-01626-8.

Figure legends

Figure 1. Research design (A) and flowchart (B) for identification of prognostic signature by immunophenotyping (IPT) to predict treatment response to immune checkpoint inhibitors (ICI) of patients with metastatic cancer.

Figure 2. Characteristics of the flow cytometry-based whole-blood prognostic immune signature (FCBPS) in the training and validation cohorts.

(A) The risk score of each metastatic cancer patient (patient ID) treated with ICI in the training cohort. **(B)** Overall survival and survival status of metastatic cancer patients in the training cohort. **(C)** Heat map of immune cell counts of metastatic cancer patients in the training cohort. **(D)** The risk score of each metastatic cancer patient treated with ICI in the validation cohort. **(E)** Overall survival and survival status of metastatic cancer patients in the validation cohort. **(F)** Heat map of immune cell counts of metastatic cancer patients in the validation cohort. pDCs: plasmacytoid dendritic cells; NKT cells: natural killer T cells; PD-1: Programmed cell death protein 1.

Figure 3. The ability of the FCBPS to predict the overall survival in the training and validation cohorts.

(A) The overall survival in training cohort stratified by the FCBPS into high- and low-risk with the P-value. **(B)** Time-dependent ROC curves of FCBPS in the training cohort. **(C)** The overall survival in validation cohort stratified by the FCBPS into high- and low-risk with the P-value. **(D)** Time-dependent ROC curves of FCBPS in the validation cohort.

Figure 4. FCBPS predicts survival benefit from ICI treatment in all metastatic cancer patients of the ST-ICI study.

(A) The overall survival in all patients stratified by the FCBPS into high- and low-risk with the P-value. **(B)** Time-dependent ROC curves of FCBPS for overall survival in all patients. **(C)** The progression-free survival in all patients stratified by the FCBPS into high- and low-risk with the P-value. **(D)** Time-dependent ROC curves of FCBPS for

progression-free survival in all patients.

Figure 5. Subgroup analysis of the FCBPS predict survival benefit of patients treated with ICI by baseline characteristics.

Subgroup analysis of the FCBPS predict overall survival **(A)** benefit and progression-free survival benefit **(B)** of patients treated with ICI. Hazard Ratio and 95% Confidence Intervals.

Table legends

Table 1. Baseline characteristics of metastatic cancer patients treated with ICI and for which immunophenotyping was performed before the second administration of ICI.

Table 2. Univariate Cox regression (p<0.2).

Table 3 . Univariate and multivariate Cox regression analysis for overall survival and progression-free survival.

Supplementary information

sFigure 1. Schematic overview of the immune cell types identified in the immunophenotyping assay. The scheme depicts the immune cell types analyzed from whole blood. The main cell types (big cells) are identified by their expression of specific cell surface molecules (pan markers). The defined cell types are excluded from the further gating steps, which allows the identification of cell types not expressing characteristic pan markers (dendritic cells, basophils). The main cell types are further divided in cell subtypes (small cells) by analyzing further surface molecules. The immune cell types and subtypes are finally analyzed for the

expression of various activation markers (CD25, CD69, CD80, CD86, PD-L1, HLA-DR, CTLA-4 and PD-1).

sFigure 2. FCBPS predict survival benefit from ICI by tumour entity.

(A) The overall survival in HNSCC patients stratified by the FCBPS into high- and low-risk with the P-value. **(B)** The overall survival in NSCLC patients stratified by the FCBPS into high- and low-risk with the P-value. **(C)** The progression-free survival in HNSCC patients stratified by the FCBPS into high- and low-risk with the P-value. **(D)** The progression-free survival in NSCLC patients stratified by the FCBPS into high- and low-risk with the P-value.

sFigure 3. FCBPS predict survival benefit from ICI by PD-L1 expression.

(A) The overall survival in patients with PD-L1 <1% stratified by the FCBPS into high- and low-risk with the P-value. **(B)** The overall survival in patients with 1% <PD-L1 < 49% stratified by the FCBPS into high- and low-risk with the P-value. **(C)** The overall survival in patients with PD-L1 >50% stratified by the FCBPS into high- and low-risk with the P-value. **(D)** The progression-free survival in patients with PD-L1 <1% stratified by the FCBPS into high- and low-risk with the P-value. **(E)** The progression-free survival in patients with 1% <PD-L1 < 49% stratified by the FCBPS into high- and low-risk with the P-value. **(F)** The progression-free survival in patients with PD-L1 >50% stratified by the FCBPS into high- and low-risk with the P-value.

sFigure 4. FCBPS predict survival benefit from ICI by non-brain metastasis.

(A) The overall survival in patients with brain metastasis stratified by the FCBPS into high- and low-risk with the P-value. **(B)** The overall survival in patients without brain metastasis stratified by the FCBPS into high- and low-risk with the P-value. **(C)** The progression-free survival in patients brain metastasis stratified by the FCBPS into high- and low-risk with the P-value. **(D)** The progression-free survival in patients without brain metastasis stratified by the FCBPS into high- and low-risk with the P-value.

sFigure 5. FCBPS predict survival benefit from ICI by age.

(A) The overall survival in age < 60yr patients stratified by the FCBPS into high- and low-risk with the P-value. **(B)** The overall survival in age ≥ 60yr patients stratified by the FCBPS into high- and low-risk with the P-value. **(C)** The progression-free survival in age < 60yr patients stratified by the FCBPS into high- and low-risk with the P-value. **(D)** The progression-free survival in age ≥ 60yr patients stratified by the FCBPS into high- and low-risk with the P-value.

sFigure 6. FCBPS predict survival benefit from ICI by gender.

(A) The overall survival in male patients stratified by the FCBPS into high- and low-risk with the P-value. **(B)** The overall survival in female patients stratified by the FCBPS into high- and low-risk with the P-value. **(C)** The progression-free survival in male patients stratified by the FCBPS into high- and low-risk with the P-value. **(D)** The progression-free survival in female patients stratified by the FCBPS into high- and low-risk with the P-value.

A

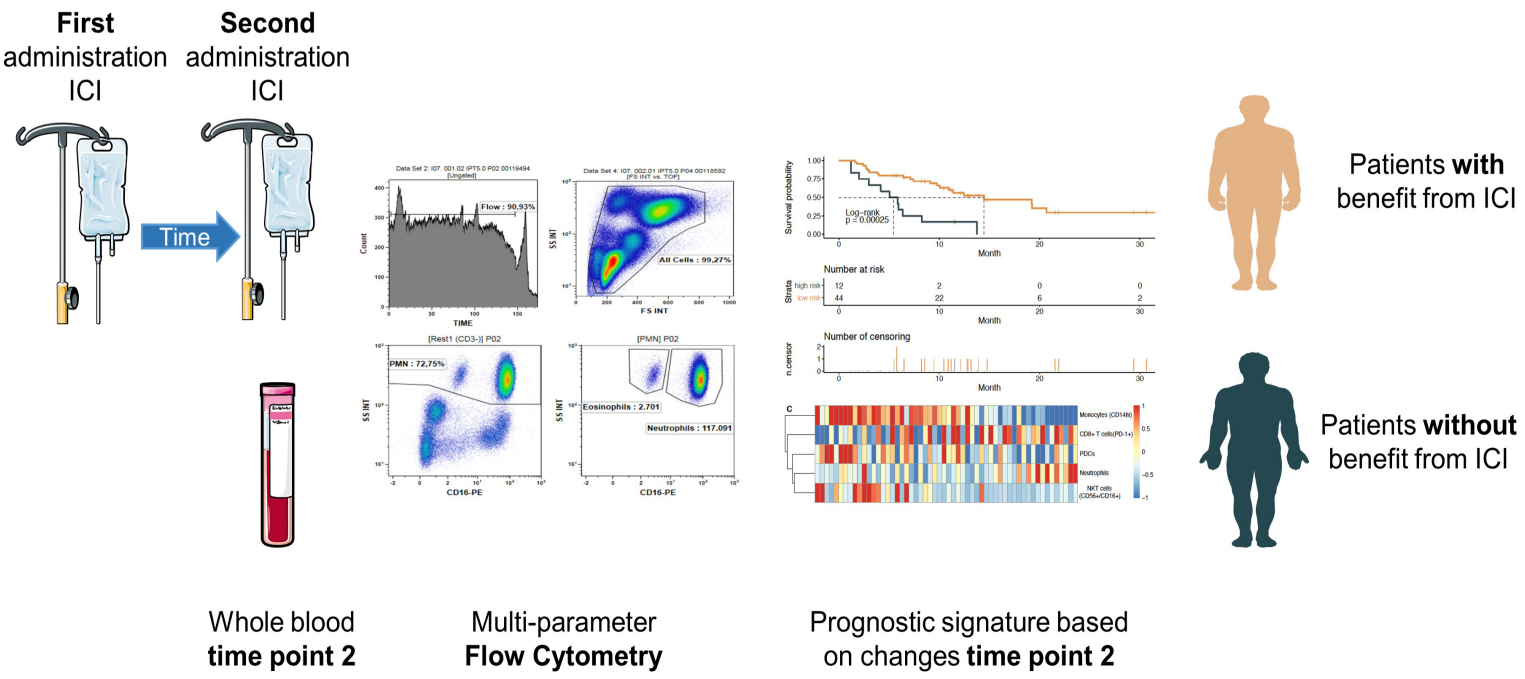
First administration ICI
Second administration ICI
Time
Flow : 90,93%
All Cells : 99,27%
PMN : 72,75%
Eosinophils : 2.701
Neutrophils : 117.091
Log-rank p = 0.00025
Number at risk
Number of censoring
Month
Patients with benefit from ICI
Patients without benefit from ICI
Whole blood time point 2
Multi-parameter Flow Cytometry
Prognostic signature based on changes time point 2

B

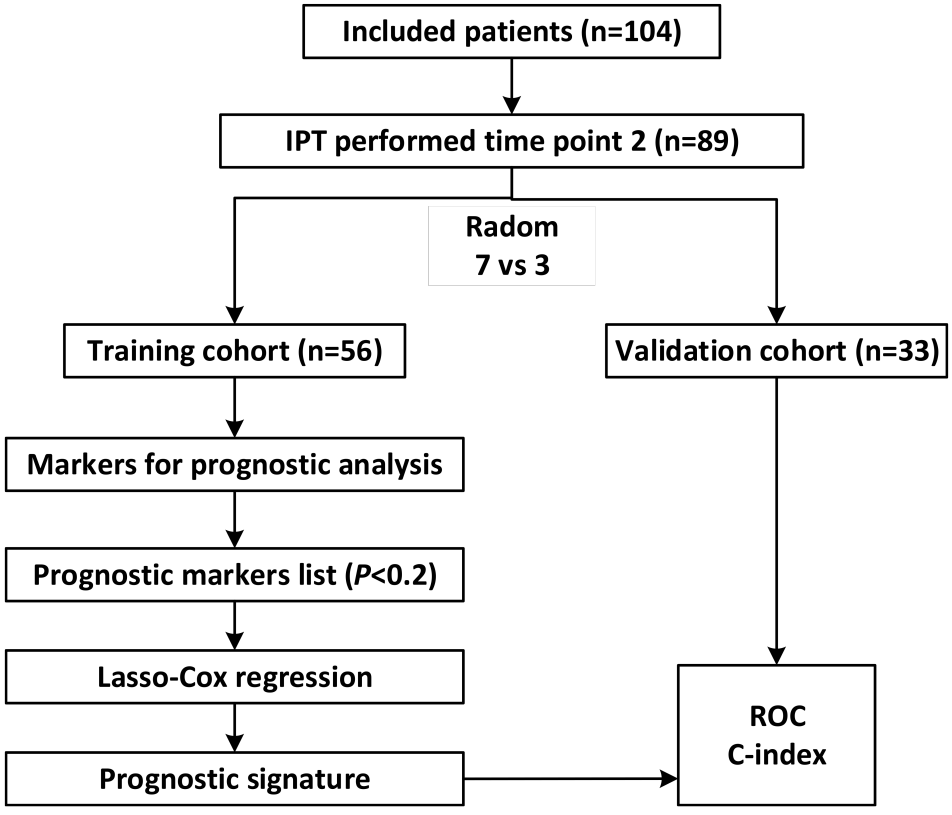
Included patients (n=104)
IPT performed time point 2 (n=89)
Radom
7 vs 3
Training cohort (n=56)
Validation cohort (n=33)
Markers for prognostic analysis
Prognostic markers list (P<0.2)
Lasso-Cox regression
Prognostic signature
ROC
C-index

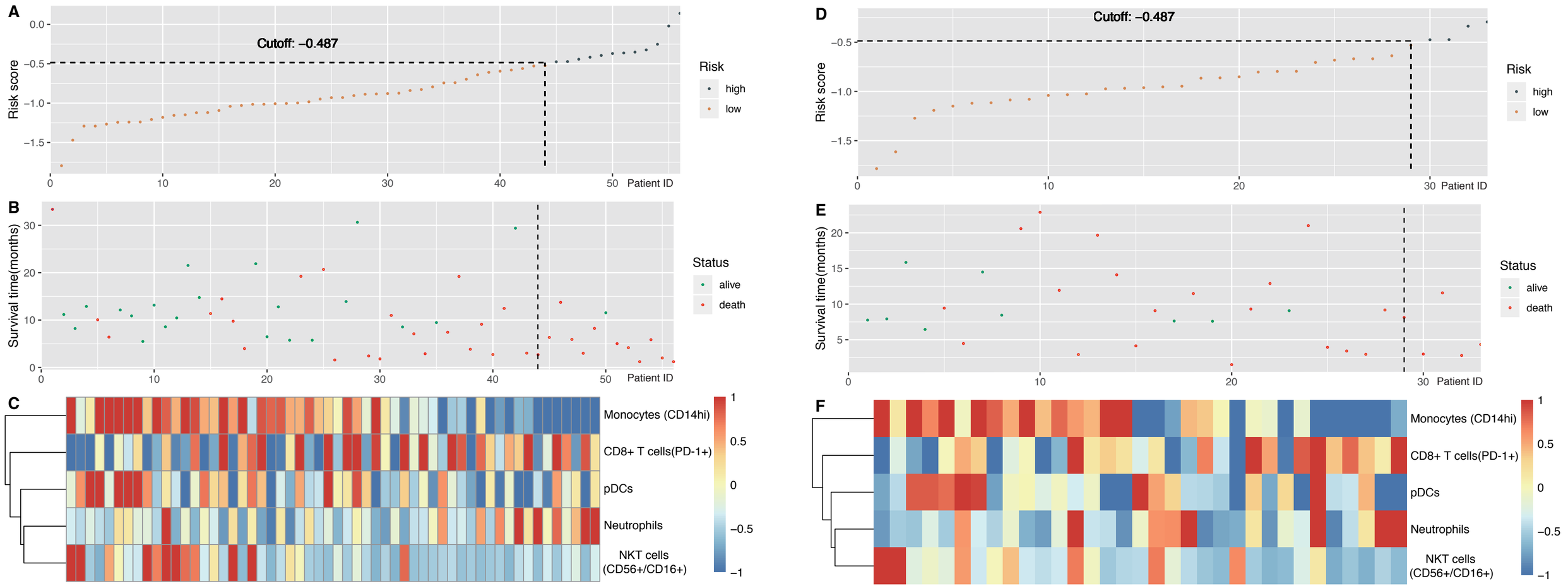
A
Cutoff: −0.487
Risk score
Patient ID
Risk
high
low
B
Survival time(months)
Patient ID
Status
alive
death
C
Monocytes (CD14hi)
CD8+ T cells(PD-1+)
pDCs
Neutrophils
NKT cells
(CD56+/CD16+)
D
Cutoff: −0.487
Risk score
Patient ID
Risk
high
low
E
Survival time(months)
Patient ID
Status
alive
death
F
Monocytes (CD14hi)
CD8+ T cells(PD-1+)
pDCs
Neutrophils
NKT cells
(CD56+/CD16+)

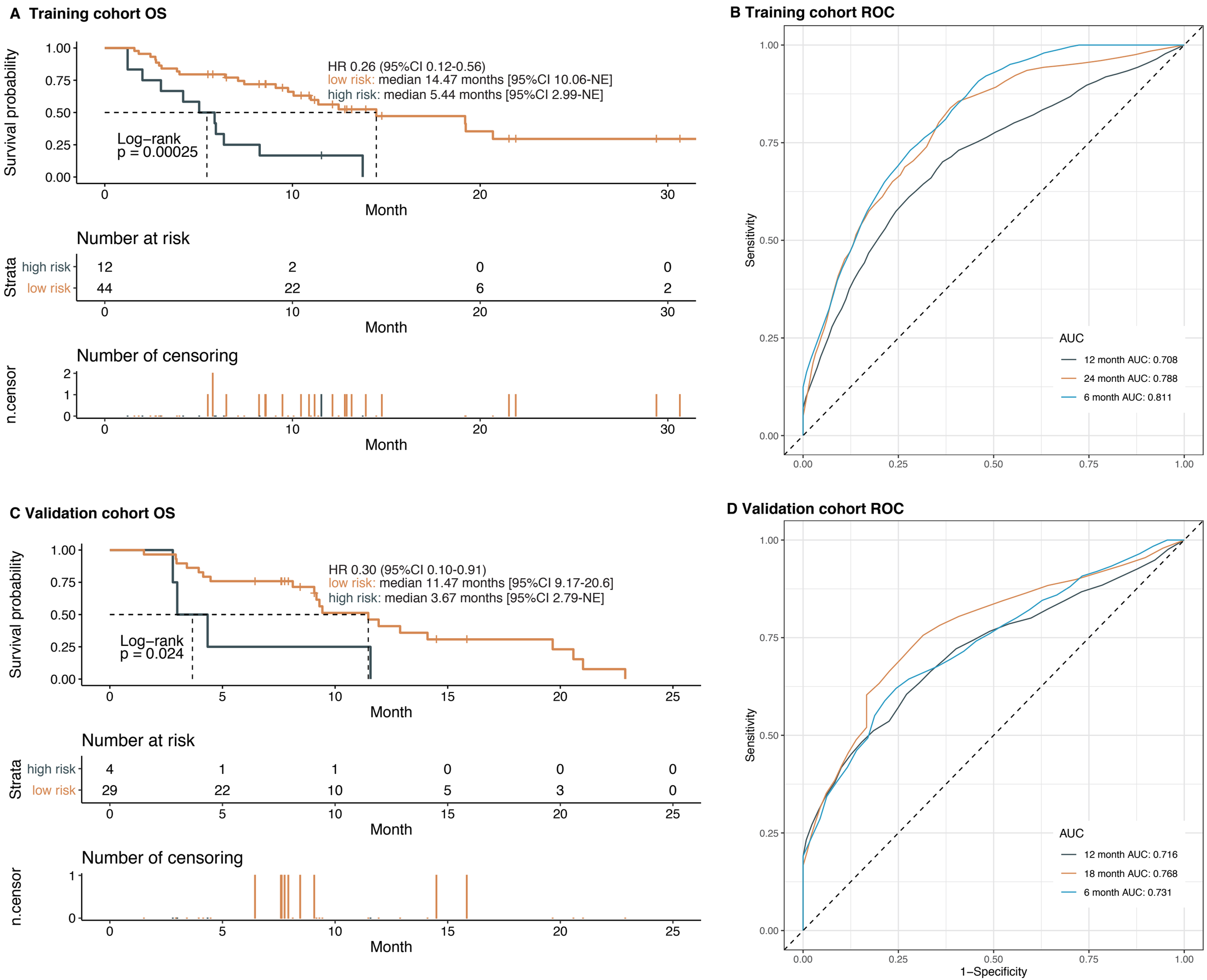
A Training cohort OS
Survival probability
HR 0.26 (95%CI 0.12-0.56)
low risk: median 14.47 months [95%CI 10.06-NE]
high risk: median 5.44 months [95%CI 2.99-NE]
Log−rank
p = 0.00025
Month
Number at risk
Strata
high risk 12 2 0 0
low risk 44 22 6 2
Number of censoring
n.censor
B Training cohort ROC
Sensitivity
AUC
12 month AUC: 0.708
24 month AUC: 0.788
6 month AUC: 0.811
C Validation cohort OS
HR 0.30 (95%CI 0.10-0.91)
low risk: median 11.47 months [95%CI 9.17-20.6]
high risk: median 3.67 months [95%CI 2.79-NE]
Log−rank
p = 0.024
high risk 4 1 1 0 0 0
low risk 29 22 10 5 3 0
D Validation cohort ROC
1−Specificity
AUC
12 month AUC: 0.716
18 month AUC: 0.768
6 month AUC: 0.731

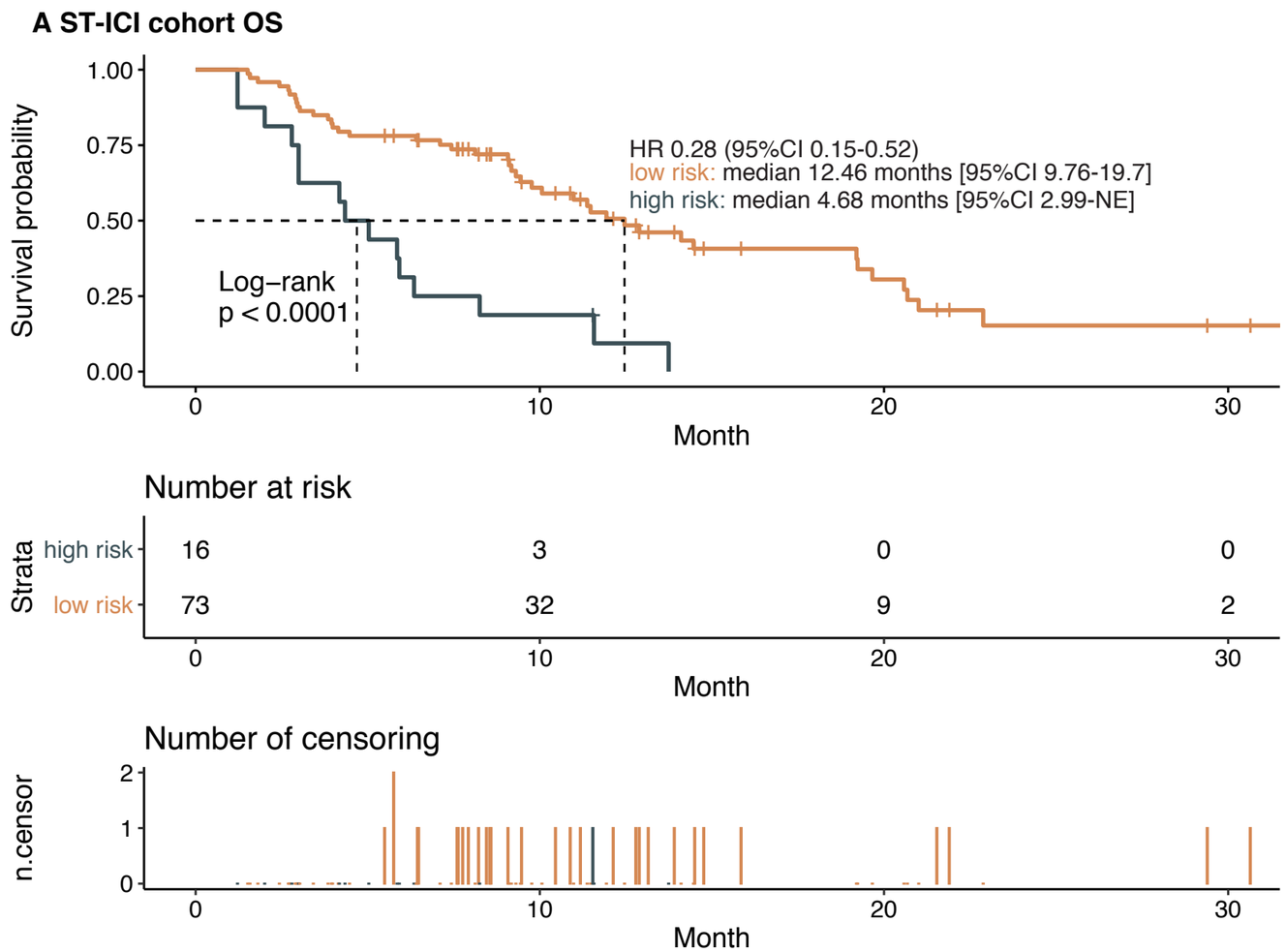
A ST-ICI cohort OS
Survival probability
1.00
0.75
0.50
0.25
0.00
HR 0.28 (95%CI 0.15-0.52)
low risk: median 12.46 months [95%CI 9.76-19.7]
high risk: median 4.68 months [95%CI 2.99-NE]
Log−rank
p < 0.0001
0
10
20
30
Month
Number at risk
Strata
high risk
low risk
16
3
0
0
73
32
9
2
Month
Number of censoring
n.censor
2
1
0
Month

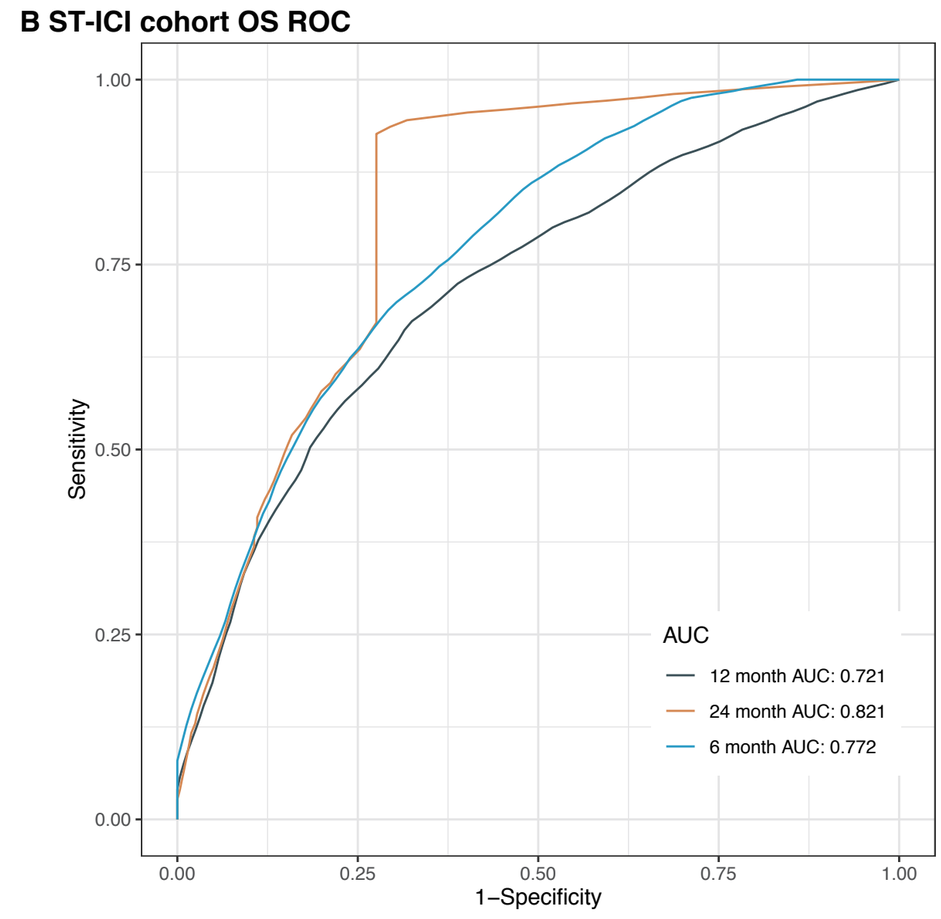
B ST-ICI cohort OS ROC
Sensitivity
1.00
0.75
0.50
0.25
0.00
1−Specificity
AUC
12 month AUC: 0.721
24 month AUC: 0.821
6 month AUC: 0.772

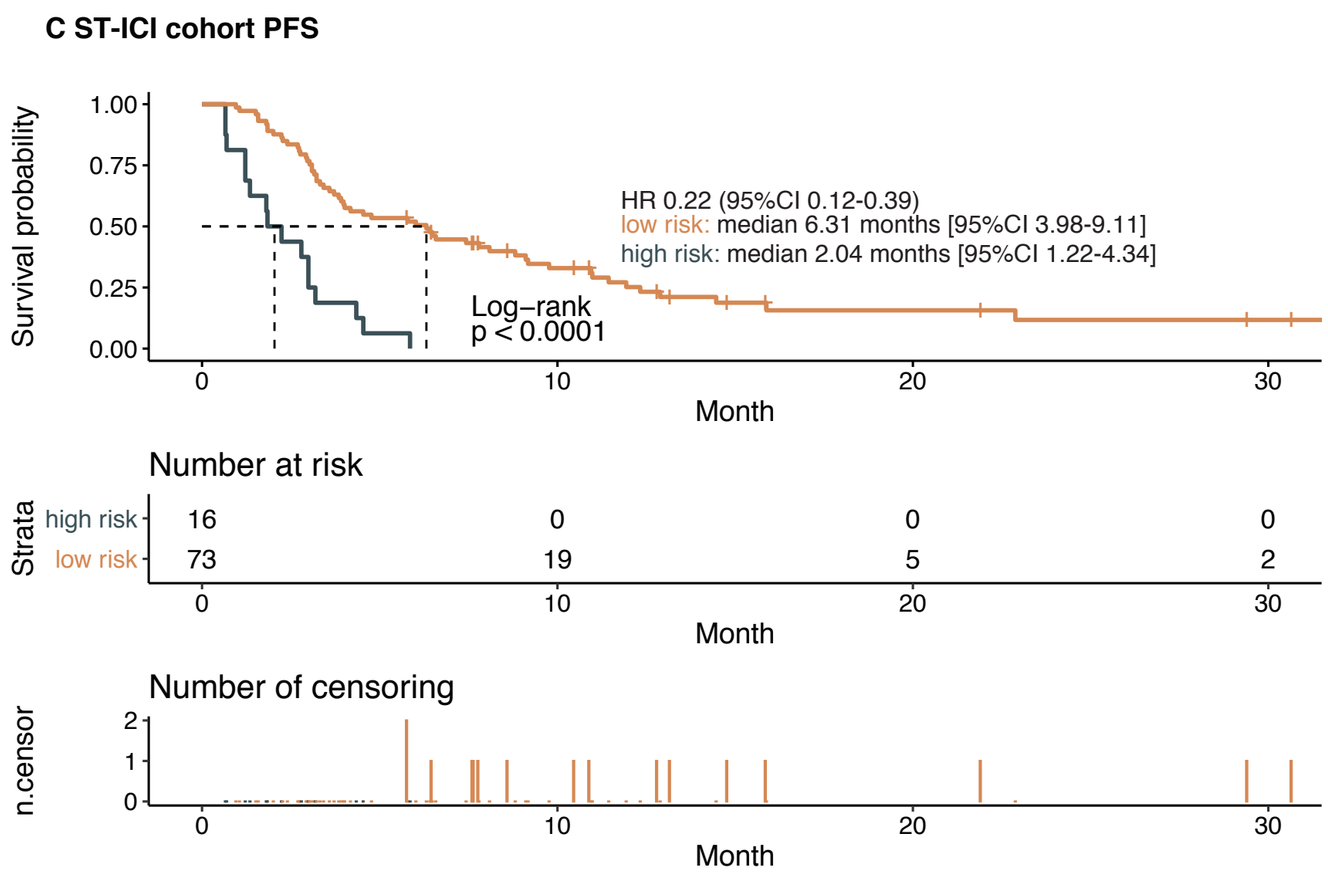
C ST-ICI cohort PFS
Survival probability
1.00
0.75
0.50
0.25
0.00
HR 0.22 (95%CI 0.12-0.39)
low risk: median 6.31 months [95%CI 3.98-9.11]
high risk: median 2.04 months [95%CI 1.22-4.34]
Log−rank
p < 0.0001
0
10
20
30
Month
Number at risk
Strata
high risk
low risk
16
0
0
0
73
19
5
2
Month
Number of censoring
n.censor
2
1
0
Month

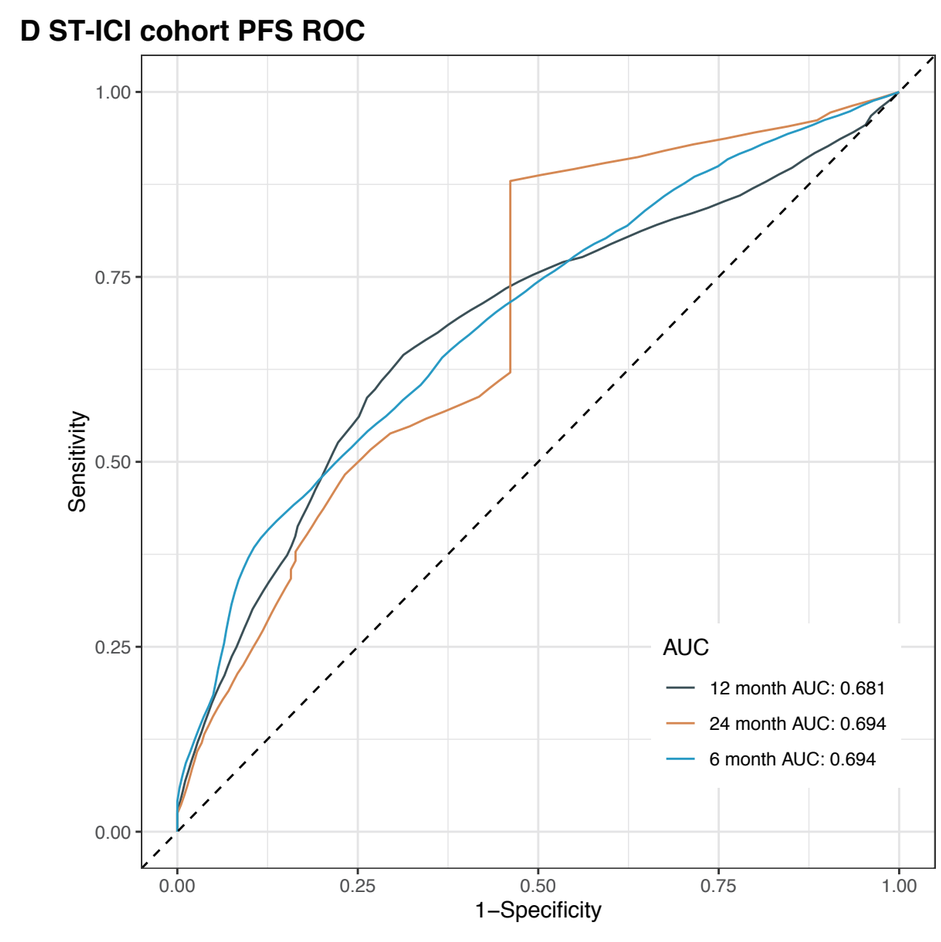
D ST-ICI cohort PFS ROC
Sensitivity
1.00
0.75
0.50
0.25
0.00
1−Specificity
AUC
12 month AUC: 0.681
24 month AUC: 0.694
6 month AUC: 0.694

A. Subgroup analysis of OS

Subgroup	Low risk (Month)	High risk (Month)	Hazard Ratio (95%CI)
All patients	**12.46**	**4.68**	**0.28 (0.15–0.52)**
Age			
Less than 60 yr	19.66	5.03	0.16 (0.05–0.48)
More than 60 yr	11.38	4.18	0.30 (0.13–0.67)
Gender			
Male	11.93	5.85	0.28 (0.14–0.59)
Female	19.66	4.34	0.28 (0.09–0.90)
Tumor entity			
HNSCC	12.89	4.34	0.39 (0.15–1.03)
NSCLC	14.47	5.44	0.19 (0.07–0.47)
Others	9.11	1.22	2.788e−10 (0–Inf)
Expression of PD–L1			
< 1%	9.07	5.03	0.45 (0.16–1.24)
1–49%	12.9	2.5	0.03 (0.01–0.20)
50–100%	14.47	5.85	0.26 (0.08–0.82)
Brain metastasis			
Yes	3.98	6.1	0.85 (0.30–2.47)
No	12.89	4.26	0.18 (0.08–0.41)

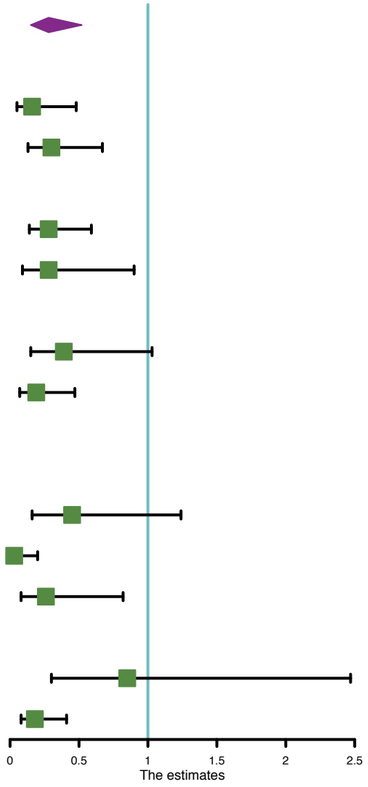

B. Subgroup analysis of PFS
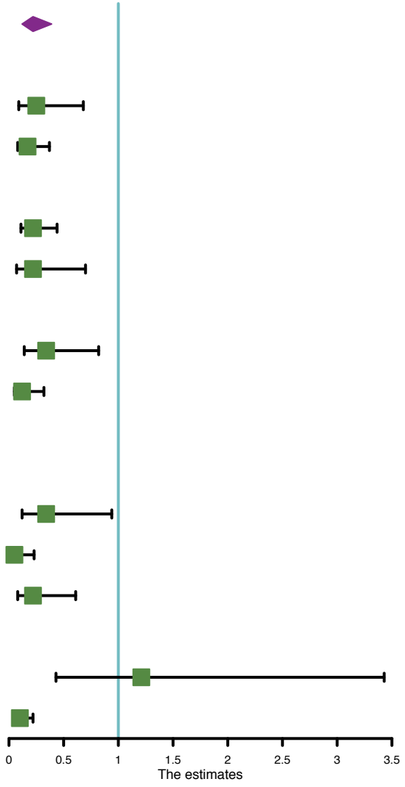
Subgroup	Low risk (Month)	High risk (Month)	Hazard Ratio (95%CI)
All patients	**6.31**	**2.04**	**0.22 (0.12–0.39)**
Age			
Less than 60 yr	7.43	2.99	0.25 (0.09–0.68)
More than 60 yr	6.02	1.81	0.17 (0.08–0.37)
Gender			
Male	5.79	2.24	0.22 (0.11–0.44)
Female	9.76	1.84	0.22 (0.07–0.70)
Tumor entity			
HNSCC	3.91	2.99	0.34 (0.14–0.82)
NSCLC	8.81	2.04	0.12 (0.05–0.32)
Others	3.42	1.22	7.578e−10 (0–Inf)
Expression of PD–L1			
< 1%	3.5	1.81	0.34 (0.12–0.94)
1–49%	9.11	0.94	0.05 (0.01–0.23)
50–100%	6.58	2.79	0.22 (0.08–0.61)
Brain metastasis			
Yes	2.4	3.09	1.21 (0.43–3.43)
No	6.58	1.28	0.10 (0.05–0.22)